



# Carbonation rate of alkali-activated concretes and high-volume SCM concretes: a literature data analysis by RILEM TC 281-CCC

Gregor J. G. Gluth · Xinyuan Ke · Anya Vollpracht · Lia Weiler · Susan A. Bernal · Martin Cyr · Katja Dombrowski-Daube · Daniel A. Geddes · Cyrill Grengg · Cassandre Le Galliard · Marija Nedeljkovic · John L. Provis · Luca Valentini · Brant Walkley

Received: 28 February 2022 / Accepted: 4 September 2022  
© The Author(s) 2022

**Abstract** The current understanding of the carbonation and the prediction of the carbonation rate of alkali-activated concretes is complicated *inter alia* by the wide range of binder chemistries used and testing conditions adopted. To overcome some of the limitations of individual studies and to identify general correlations between mix design parameters and carbonation resistance, the RILEM TC 281-CCC ‘Carbonation of Concrete with Supplementary Cementitious Materials’ Working Group 6 compiled

and analysed carbonation data for alkali-activated concretes and mortars from the literature. For comparison purposes, data for blended Portland cement-based concretes with a high percentage of SCMs ( $\geq 66\%$  of the binder) were also included in the database. The analysis indicates that water/CaO ratio and water/binder ratio exert an influence on the carbonation resistance of alkali-activated concretes; however, these parameters are not good indicators of the carbonation resistance when considered

This article was prepared within the framework of RILEM TC 281-CCC. The article has been reviewed and approved by all members of the TC.

## TC Membership

*Chair:* Nele De Belie

*Deputy Chair:* Susan A. Bernal

*Members:* Natalia Alderete, Carmen Andrade, Ueli Angst, Tushar Bansal, Véronique Baroghel-Bouny, Muhammed P. A. Basheer, Susan A. Bernal, Hans D. Beushausen, Leon Black, Aires Camões, Servando Chinchón-Payá, Özlem Cizer, Gisela Paola Cordoba, Martin Cyr, Patrick Dangla, Nele De Belie, Yuvaraj Dhandapani, Katja Dombrowski-Daube, Vilma Ducman, Yogarajah Elakneswaran, Jan Elsen, Juan Manuel Etcheverry, Miren Etxeberria, Ana M. Fernández-Jiménez, Lander Frederickx, Isabel Fuencisla Saez del Bosque, Inês Garcia Lodeiro, Daniel Geddes, Christoph Gehlen, Mette Geiker, Guoqing Geng, Bahman Ghiassi, Gregor Gluth, Cyrill Grengg, Elke Gruyaert, R. Doug Hooton, Bruno Huet, Andres Idiart, Ivan Ignjatović, Kei-ichi Imamoto, Shiju Joseph, Siham Kamali-Bernard, Antonis Kanellopoulos, Xinyuan Ke, Sylvia Kessler, Heejeong Kim, Arto Köliö, Cassandre Le Galliard, Juan Li, Ning Li, Tung-Chai Ling, Qing-Feng Liu, Zhiyuan Liu, Barbara Lothenbach, Isabel Martins, José Fernando Martirena-Hernández, César Medina Martínez, Fabrizio Moro,

Shishir Mundra, Marija Nedeljkovic, Kolawole A. Olonade, Jose Pacheco, Christian Paglia, Angel Palomo, Ravi Patel, Janez Perko, Quoc Tri Phung, John L. Provis, Francisca Puertas, Nuria Rebolledo, Marlene Sakoparnig, Javier Sanchez Montero, Francesco Santoro, Sriram Pradeep Saridhe, Karen Scrivener, Marijana Serdar, Zhenguo Shi, Kosmas K. Sideris, Ruben Snellings, Matteo Stefanoni, Charlotte Thiel, Karl-Christian Thienel, Michael D. A. Thomas, Ilda Tole, Luca Valentini, Philip Van den Heede, Hanne Vanoutrive, Yury Andrés Villagrán Zaccardi, Talakokula Visalakshi, Anya Vollpracht, Stefanie von Greve-Dierfeld, Brant Walkley, Fazhou Wang, Ling Wang, Jinxin Wei, Lia Weiler, Bei Wu, Yan Yao, Guang Ye, Maciej Zajac, Zengfeng Zhao, Semion Zhutovskiy.

**Supplementary Information** The online version contains supplementary material available at <https://doi.org/10.1617/s11527-022-02041-4>.

G. J. G. Gluth (✉)  
Division 7.4 Technology of Construction Materials,  
Bundesanstalt für Materialforschung und -prüfung  
(BAM), Berlin, Germany  
e-mail: gregor.gluth@bam.de



individually. A better indicator of the carbonation resistance of alkali-activated concretes under conditions approximating natural carbonation appears to be their  $\text{water}/(\text{CaO} + \text{MgO}_{\text{eq}} + \text{Na}_2\text{O}_{\text{eq}} + \text{K}_2\text{O}_{\text{eq}})$  ratio, where the subscript 'eq' indicates an equivalent amount based on molar masses. Nevertheless, this ratio can serve as approximate indicator at best, as other parameters also affect the carbonation resistance of alkali-activated concretes. In addition, the analysis of the database points to peculiarities of accelerated tests using elevated  $\text{CO}_2$  concentrations for low-Ca alkali-activated concretes, indicating that even at the relatively modest concentration of 1%  $\text{CO}_2$ , accelerated testing may lead to inaccurate predictions of the carbonation resistance under natural exposure conditions.

**Keywords** Alkali-activated materials · Durability · Carbonation · Accelerated testing

## 1 Introduction

The carbonation of cementitious materials is a degradation phenomenon taking place when  $\text{CO}_2$  from the air enters the material, promoting chemical reactions that modify the chemistry and microstructure of the

carbonated binders, potentially leading to the corrosion of embedded steel reinforcement. This degradation mechanism can have significant consequences, in many cases being the limiting factor for the service life of reinforced concrete structures. For concretes based on conventional cements (Portland and blended Portland cements), the water-to-reactive  $\text{CaO}$  ( $w/\text{CaO}_{\text{reactive}}$ ) ratio has been found to be the major parameter determining their carbonation resistance [1, 2]. Related to this ratio are concepts that involve the water-to-binder ( $w/b$ ) ratio and the clinker content [3] as well as the  $k$ -value concept described in EN 206 [4]. However, for concretes and mortars based on alkali-activated binders and other alternative cements these approaches seem to be not applicable without modifications [5, 6]. Alternative approaches that apply specifically to alkali-activated concretes are currently not available, mainly because the mechanisms and factors determining the carbonation resistance of alkali-activated concretes are not yet completely understood. This is partly due to the wide range of chemistries of alkali-activated binders, notably their variability in  $\text{CaO}$  content, and the fact that individual carbonation studies are generally limited to only a few mix designs, curing conditions and exposure conditions [7].

---

X. Ke  
Department of Architecture and Civil Engineering, The University of Bath, Bath, UK

A. Vollpracht · L. Weiler  
Institute of Building Materials Research, RWTH Aachen University, Aachen, Germany

S. A. Bernal  
School of Civil Engineering, The University of Leeds, Leeds, UK

M. Cyr  
Laboratoire Matériaux Et Durabilité Des Constructions (LMDC), Université de Toulouse, Toulouse, France

K. Dombrowski-Daube  
Institut für Bergbau und Spezialtiefbau, Technische Universität Bergakademie Freiberg, Freiberg, Germany

D. A. Geddes · C. Le Galliard · J. L. Provis  
Department of Materials Science and Engineering, The University of Sheffield, Sheffield, UK

C. Grengg  
Institute of Applied Geosciences, Graz University of Technology, Graz, Austria

M. Nedeljkovic  
Faculty of Civil Engineering and Geosciences, Delft University of Technology, Delft, The Netherlands

L. Valentini  
Department of Geosciences, University of Padua, Padua, Italy

B. Walkley  
Department of Chemical and Biological Engineering, The University of Sheffield, Sheffield, UK



To address these issues, the RILEM TC 281-CCC Working Group 6 compiled carbonation data for a wide range of alkali-activated concretes and mortars from the literature. This has been done with the aim of resolving the shortcomings of individual studies and to identify general correlations between mix design parameters of alkali-activated concretes and mortars, and their carbonation resistance. For comparison purposes, data for blended Portland cement-based concretes and mortars with a high percentage of supplementary cementitious materials (SCMs) in the binder were included in the database. In this report, the database, the assumptions made in the evaluation of the data, the analysis results and their implications are presented.

## 2 Data inventory and processing

### 2.1 Data inventory

To create the database, the literature was searched for studies that report carbonation depth ( $d_c$ )-versus-carbonation duration ( $t$ ) data for alkali-activated concretes or mortars, for concretes or mortars based on blended Portland cements with at least 70%<sup>1</sup> SCMs in the binder, as well as for concretes or mortars based on CEM III/B [66–80% ground granulated blast furnace slag (GGBS) in the binder according to EN 197–1]. Only data obtained at controlled relative humidity (conditions approximating indoor or “sheltered” natural carbonation, and accelerated carbonation) were included in the database. Results for unsheltered natural exposure were not considered, because the degree of saturation of the pore systems of the exposed concretes is not controlled in these experiments, complicating the comparison and interpretation of the results. Carbonation data for pastes were not considered, as the potential effects of aggregates (particularly, but not solely, due to the presence of the microstructurally distinct interfacial transition zone between paste and aggregate) on the

carbonation coefficient would not be observed for these. Studies with incomplete or internally inconsistent information about the mix design or the test conditions were also excluded from the database.

In most of the studies, the carbonation depths were determined by spraying a phenolphthalein solution (usually with a concentration of 1%) on fracture surfaces; in one case alizarin yellow R was used as the indicator, and in another case thin sections were examined. It is noted that there are difficulties and open questions regarding the phenolphthalein-spraying method for the determination of the carbonation depths of alkali-activated concretes, which may influence the outcomes of carbonation testing [8]. However, this method is currently the most widely used and, thus, the present analysis had to rely on the results obtained with this method to be able to include a significant number of studies.

The mix designs of the concretes or mortars, the chemical compositions of the binders (solid precursors and activators), the physical properties of the constituents, the compressive strengths of the cured materials as well as curing, preconditioning and carbonation conditions were included in the database together with the respective carbonation-depth data. The full database is provided in the Electronic Supplementary Material.

For the present purpose, ‘GGBS-based AAC’ were defined as alkali-activated concretes/mortars in which the most abundant (by mass) component of the binder was GGBS. ‘FA- and MK-based AAC’ are correspondingly defined as alkali-activated concretes/mortars with fly ash (FA) or metakaolin (MK) as the most abundant binder component; only one of the twelve pertinent mixes in the database was based on MK. Mixes in which GGBS and FA were present in equal amounts in the binder, were assigned to the GGBS-based AAC. The term ‘other AAC’ is used to denote alkali-activated concretes/mortars with binders based on municipal solid waste incineration (MSWI) bottom ash, silico-manganese slag or natural pozzolans. Two hybrid cements, *i.e.* cements containing Portland clinker as well as a second activator, were assigned to this class as well. Most of the AAC in the database were activated with sodium silicate solutions, while fewer were activated with NaOH, Na<sub>2</sub>CO<sub>3</sub>, or a mixture of sodium silicate and Na<sub>2</sub>CO<sub>3</sub>. In some cases, portlandite [Ca(OH)<sub>2</sub>] or gypsum [CaSO<sub>4</sub>·2H<sub>2</sub>O] were employed as additional activators.

<sup>1</sup> In the present report, all ratios and fractions pertaining to the compositions of the materials are given as mass ratios (or equivalent mass ratios; see Sect. 2.2) and mass fractions, respectively, unless indicated otherwise by giving a unit other than kg/kg in parentheses [for example, total binder content (kg/m<sup>3</sup>), activator modulus or SiO<sub>2</sub>/Na<sub>2</sub>O molar ratio (mol/mol)]. Gas concentrations are given as volume fractions.

The compressive strengths of the alkali-activated concretes and mortars in the database differed widely. A consideration of the parameters determining the strength of these materials is beyond the scope of the present article, but influences on the compressive strength of alkali-activated concretes have been discussed extensively in the literature (e.g., Ref. [9]). However, there is no correlation apparent between the compressive strength of these materials and their durability-related transport parameters, such as chloride penetration coefficients [8]; thus, a classification or preselection of the concretes/mortars based on their compressive strength or strength class was not conducted for the present analysis.

The majority of the materials based on blended Portland cements in the database are concretes (68 concretes, six mortars); these will be collectively referred to as ‘BCC’ below. The SCMs in these materials were GGBS and/or FA; in one case, a natural pozzolan was added to a CEM III/B.

The database contains data for 125 GGBS-based AAC [6, 8, 10–31]; 12 FA- or MK-based AAC [8, 32–36]; 18 other AAC [36–40]; and 74 BCC [1, 2, 6, 16, 29, 41–52]. A plot of the SCM fractions of the binders of the materials (including the compounds dissolved in the activator solution as part of the binder in the calculation) is shown in Fig. 1.; the plot does not contain the 20 mixes based on CEM III/B with no exact specification of the GGBS content.

For most of the concretes/mortars, either data for carbonation approximating natural exposure, or data for accelerated carbonation were available; for a limited number of materials, data for both conditions were reported.

## 2.2 Data evaluation

The carbonation resistance of concretes and mortars is commonly described by a single parameter, the carbonation coefficient ( $k_c$ ) [4]. The definition of  $k_c$  and its computation from experimental data is based on Fick’s first law of diffusion, and it implies that the carbonation rate of cementitious materials can be accurately described by the square-root-of-time law [53]. As has been discussed previously [5, 18, 20], this is likely not true for all alkali-activated materials, since in these materials the carbonation rate is influenced to a great extent by the reactions that take place, and it is, thus, not purely diffusion-controlled.

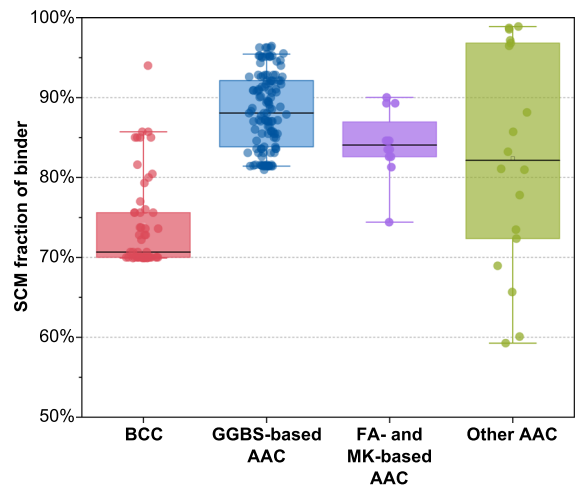


**Fig. 1** SCM fractions of the binders of the mixes included in the database. ‘Binder’ refers to the solid starting materials and the oxides ( $\text{Na}_2\text{O}$ ,  $\text{SiO}_2$  etc.) dissolved in the activator solution combined. Twenty additional blended-cement concretes/mortars (BCC) based on CEM III/B (66–80% GGBS in binder) are not included in the plot. *Black lines* represent the medians; *boxes* represent the ranges between the 25% percentile and the 75% percentile; and the *whiskers* represent the 5% percentiles and the 95% percentiles

However, to create an internally consistent dataset with values that can be compared between AAC and BCC,  $k_c$  was calculated in the usual manner for all materials in the present analysis. The thus obtained results demonstrated limitations of this approach when applied to alkali-activated materials, as will be shown below (Sect. 3.2).

When only one  $d_c$ -versus- $t$  value was given for a material tested at specific carbonation conditions, the carbonation coefficient was calculated as  $k_c = d_c/\sqrt{t}$ , meaning that  $d_c = 0$  mm at  $t = 0$  d was implicitly assumed. When multiple  $d_c$ -versus- $t$  values were available for a material tested under specific carbonation conditions, the carbonation coefficient was obtained by fitting a linear function to all available data points plotted as  $d_c(\sqrt{t})$  up to  $t = 365$  d (or up to 393 d in four cases). If that fit yielded a positive intercept with the ordinate, the slope of the function was used as  $k_c$  for the evaluation. If the fit yielded a negative intercept with the ordinate (*i.e.* a negative carbonation depth at  $t = 0$  d, which would be unphysical), the fit was repeated with the linear function forced through the origin of the coordinates, and the value thus obtained was used. It is noted that the assumption of  $d_c = 0$  mm at  $t = 0$  d is not necessarily

true, particularly for materials based on alkali-activated binders or blended cements, which can show some surface carbonation during curing and/or conditioning prior to testing [8, 54]. However, in the absence of carbonation-depth data for the start of the exposure to CO<sub>2</sub>, an assumption about  $d_c$  at  $t = 0$  d had to be made.

The dataset resulting from the round robin testing programme of RILEM TC 247-DTA [8] were treated as if they were obtained in a single laboratory, using the average of the carbonation depths at given exposure times, obtained in the participating institutes. However, the  $d_c$  values obtained in laboratory *G* in that testing programme were not included in the present analysis, because this laboratory had employed a curing regime that differed from the curing used in the other participating laboratories. The coefficient of variation (COV) of the  $d_c$  in the reduced dataset was in the range 21.2–42.1% for carbonation under conditions approximating indoor/sheltered natural exposure, and 1.0–45.4% for accelerated carbonation. To translate these uncertainties into the uncertainty of the resulting  $k_c$ , it was assumed that the COV of the latter was 40%, *i.e.* the standard deviation (s.d.) of the carbonation coefficient was estimated to be  $\text{s.d.} = 0.40 \times k_c$ .

In the discussion that follows,  $k_{c\text{-nat}}$  will be used as the symbol for carbonation coefficients obtained under conditions approximating natural carbonation (indoor/sheltered), and  $k_{c\text{-acc}}$  will be used as the symbol for carbonation coefficients obtained under accelerated conditions. If the coefficient refers to a specified CO<sub>2</sub> concentration (or range), this will be noted in brackets (*e.g.*,  $k_{c\text{-acc}}[1\%]$  or  $k_{c\text{-acc}}[3\text{--}4\%]$ ).

From the mix designs of the concretes/mortars and the chemical compositions of their constituents, several parameters that may be hypothesised to exert an influence on the carbonation rate were computed. These parameters included the  $w/\text{CaO}$  ratio, where  $w$  is the mass of water in the concrete/mortar, and CaO is the mass of CaO in the binder paste of the mortar/concrete, including the contributions from the solid binder starting materials (*e.g.*, GGBS) as well as from any compounds added as part of the activator. Analogously, the Na<sub>2</sub>O, K<sub>2</sub>O, and MgO contents refer to the respective masses of these oxides in the solid binder starting materials and in the activator combined. No attempt was made to discriminate “reactive” and “non-reactive” oxides (*cf.* Refs. [1, 2, 55]) in

the paste, as the information given in the reports containing the carbonation data was usually not sufficient to calculate these fractions with reasonable accuracy. However, inspection of the mix designs of the concretes/mortars in the database and the information given in the associated reports indicated that the majority of the alkali metals and alkaline-earth metals in the binder starting materials can be considered “reactive”, since the employed starting materials were generally of a type (GGBS, FA, MK) that typically contains only low fractions of these elements in potentially insoluble, crystalline compounds. For the concretes/mortars classified as ‘other AAC’ this assumption may be somewhat less justified, *i.e.* for these materials the oxide masses used for the computations might reflect the “reactive” oxide fraction less accurately, but detailed analysis of this point is beyond the scope of the current discussion.

For a combined consideration of the alkali metal and alkaline-earth metal oxides in the binder pastes, the masses of Na<sub>2</sub>O, K<sub>2</sub>O, and MgO were converted to “equivalent” masses (designated Na<sub>2</sub>O<sub>eq</sub>, K<sub>2</sub>O<sub>eq</sub>, and MgO<sub>eq</sub>, respectively) by multiplying them by the ratio of the molar mass of CaO to the molar mass of the respective oxide; for example,  $\text{Na}_2\text{O}_{\text{eq}} = \text{Na}_2\text{O} \cdot M_{\text{CaO}} / M_{\text{Na}_2\text{O}}$ . Through this conversion, the equivalent masses reflect the theoretical maximum CO<sub>2</sub> binding capacity of the respective oxides, analogous to the binding capacity of CaO on a molar basis. It is noted that a simplified analysis of the database using the uncorrected fractions of Na<sub>2</sub>O, K<sub>2</sub>O, and MgO yields similar conclusions as the analysis using the converted values presented in the following sections. This is because the conversion ratios are in the range 0.60–1.39, *i.e.* in a rather narrow range around unity, and, therefore, the error introduced by the use of uncorrected values is low compared to the general scatter of the data.

Several other parameters of the mix designs of the concretes/mortars were also evaluated. For all calculations, the total binder content of the concretes/mortars was defined as including the dissolved activator compounds (*e.g.*, Na<sub>2</sub>O and SiO<sub>2</sub> in a sodium silicate solution). This definition was followed also for the calculation of the  $w/b$  ratios of the concretes/mortars, *i.e.*,  $b$  in this ratio represents the total binder mass including the dissolved activator compounds.

### 3 Results and discussion

#### 3.1 Carbonation under conditions approximating natural exposure

Figure 2 shows a plot of the carbonation resistance of the concretes/mortars under conditions approximating natural carbonation  $k_{c-nat}$  versus the  $w/CaO$  ratio of their binders. It is evident that the carbonation resistance of alkali-activated concretes and mortars cannot be predicted based on their  $w/CaO$  ratio alone. The FA-based AAC, and particularly the MK-based AAC (see also Supplementary Fig. S1 in the Electronic Supplementary Material), deviate considerably from a linear relationship that might otherwise be considered for the data from the more Ca-rich binders (BCC- and GGBS-based AAC) in the plot. A plot of the data for the GGBS-based AAC alone (Fig. 3) reveals that also within this class of materials there is not a clear a correlation between  $k_{c-nat}$  and  $w/CaO$ . As GGBS typically contains significant amounts of MgO (usually in the range 5–14 wt.%), it might be conjectured that a correlation could be more evident when the ratio  $w/(CaO + MgO_{eq})$  is considered. However, the present dataset does not yield a significant improvement when MgO is considered in

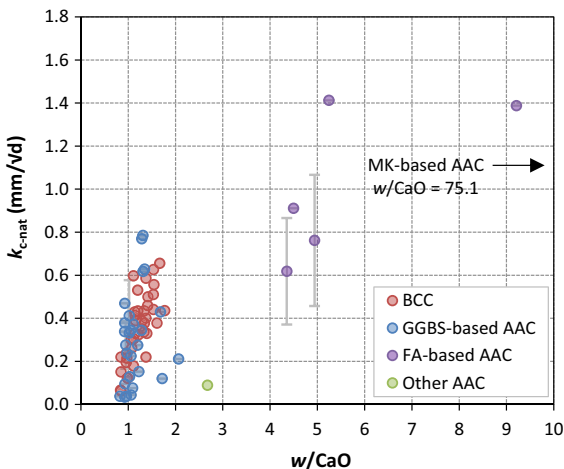


**Fig. 2** Carbonation coefficients obtained under conditions approximating natural carbonation (indoor/sheltered) versus  $w/CaO$  ratio. The data point for the MK-based AAC with  $w/CaO = 75.1$  and  $k_{c-nat} = 1.1 \text{ mm}/\sqrt{d}$  is outside the displayed range. Error bars represent the estimated s.d. of the results obtained in the round robin testing programme by RILEM TC 247-DTA

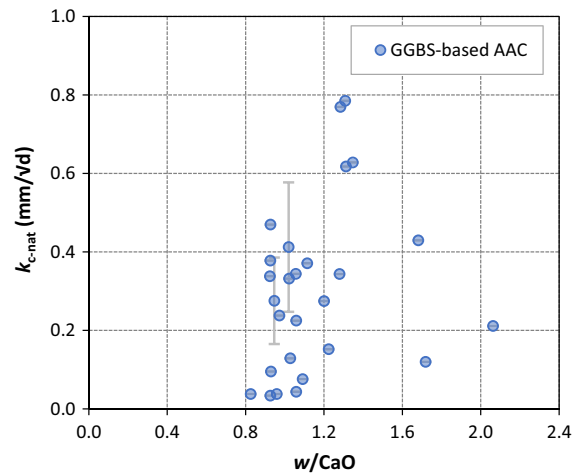


**Fig. 3** Carbonation coefficients of the GGBS-based AAC obtained under conditions approximating natural carbonation (indoor/sheltered) versus  $w/CaO$  ratio. Error bars represent the estimated s.d. of the results obtained in the round robin testing programme by RILEM TC 247-DTA

addition to CaO in this way (Supplementary Figs. S2 and S3).

Within the group of BCC, a reasonable correlation between  $k_{c-nat}$  and  $w/CaO$  was observed (coefficient of determination  $R^2 = 0.5484$ ; Fig. 4). This finding is in line with previous assessments [1, 2, 4] and extends these previous findings to blended cement concretes with particularly high SCM fractions (66–94%) in the binder. It is noted that a correlation between  $k_{c-nat}$  and  $w/CaO$  can only be expected if CaO is approximately

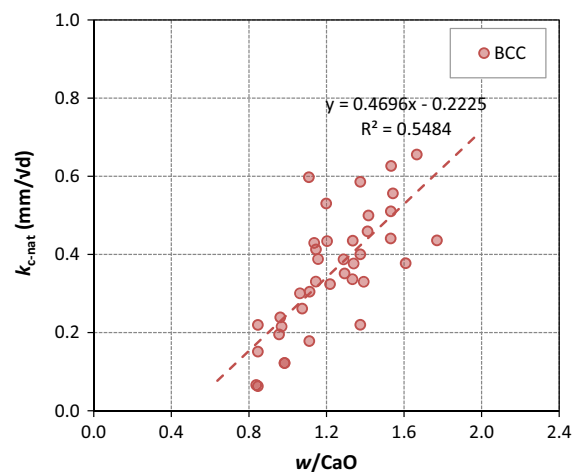


**Fig. 4** Carbonation coefficients of the BCC obtained under conditions approximating natural carbonation (indoor/sheltered) versus  $w/CaO$  ratio

proportional to  $\text{CaO}_{\text{reactive}}$ , which is assumed to be the case for the present database, as discussed in Sect. 2.2. This assumption is possibly less likely to be valid for BCC than for GGBS-based AAC, as the two distinct sources of CaO in the slag-rich Portland cement blends (clinker and slag) will provide a clearly bimodal distribution of CaO reactivity, whereas the CaO in a GGBS-based AAC mix is all from a single source. As with the GGBS-based AAC, there was no improvement in the correlation when considering  $w/(\text{CaO} + \text{MgO}_{\text{eq}})$  instead of  $w/\text{CaO}$  ( $R^2 = 0.5061$ ; Supplementary Fig. S4).

The observation that the AAC do not follow the same trend as the BCC as regards the relationship between  $k_{\text{c-nat}}$  and  $w/\text{CaO}$  can be attributed to the fact that in alkali-activated binders, carbonation is determined to a large extent by the amount of alkali ions present in the pore solution [5, 56]. Indeed, in a plot considering all alkali metals and alkaline-earth metals in the binders, *i.e.*  $k_{\text{c-nat}}$  versus  $w/(\text{CaO} + \text{MgO}_{\text{eq}} + \text{Na}_2\text{O}_{\text{eq}} + \text{K}_2\text{O}_{\text{eq}})$  (Fig. 5), the FA-based AAC cluster more closely together with the BCC and the GGBS-based AAC than in the plot of  $k_{\text{c-nat}}$  versus  $w/(\text{CaO})$ , and a correlation between  $k_{\text{c-nat}}$  and  $w/(\text{CaO} + \text{MgO}_{\text{eq}} + \text{Na}_2\text{O}_{\text{eq}} + \text{K}_2\text{O}_{\text{eq}})$  can be discerned, although the scatter of the data is substantial. In particular, there is a significant deviation between the  $w/(\text{CaO} + \text{MgO}_{\text{eq}} + \text{Na}_2\text{O}_{\text{eq}} + \text{K}_2\text{O}_{\text{eq}})$  ratios of

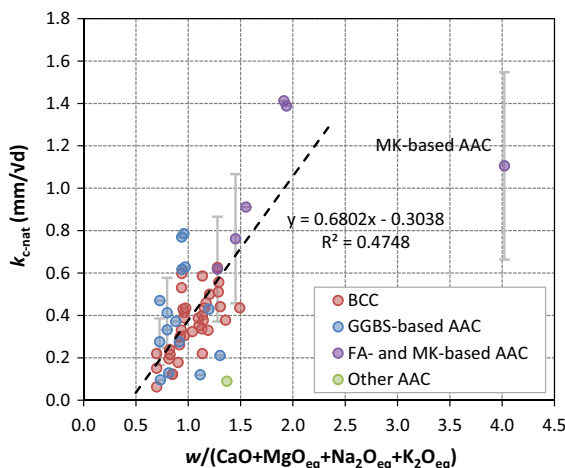


**Fig. 5** Carbonation coefficients obtained under conditions approximating natural carbonation (indoor/sheltered) versus  $w/(\text{CaO} + \text{MgO}_{\text{eq}} + \text{Na}_2\text{O}_{\text{eq}} + \text{K}_2\text{O}_{\text{eq}})$  ratio. The dashed line is a linear fit through all data points except the MK-based AAC. Error bars represent the estimated s.d. of the results obtained in the round robin testing programme by RILEM TC 247-DTA

the MK-based AAC and the FA-based AAC, although both exhibit  $k_{\text{c-nat}}$  in the range approx. 0.6–1.4 mm/ $\sqrt{d}$ . This demonstrates that additional parameters not captured in this analysis influence the carbonation resistance of these concretes.

A linear regression of all data points except the MK-based AAC yields  $R^2 = 0.4748$  (Fig. 5). The obtained linear function yields an intercept with the abscissa (*i.e.*  $k_{\text{c-nat}} = 0.0$  mm/ $\sqrt{d}$ ) at  $w/(\text{CaO} + \text{MgO}_{\text{eq}} + \text{Na}_2\text{O}_{\text{eq}} + \text{K}_2\text{O}_{\text{eq}}) = 0.45$ . For conventional cementitious materials (BCC in the present study), an intercept at a value higher than zero can be rationalised by the fact that their capillary pore system will theoretically become discontinuous at a porosity of 18 vol.% [57], which corresponds to a degree of hydration of 86% for Portland cement at  $w/b = 0.50$ , or a degree of hydration of 57% at  $w/b = 0.35$  [57] (see also Ref. [58]), which is equivalent to a  $w/(\text{CaO} + \text{MgO}_{\text{eq}} + \text{Na}_2\text{O}_{\text{eq}} + \text{K}_2\text{O}_{\text{eq}})$  ratio in the range approx. 0.6–1.1. A discontinuous pore system inhibits the ingress of  $\text{CO}_2$ , thus strongly decreasing the rate of carbonation. Since the reactions and hardening of alkali-activated materials also involve the formation of (hydrated) reaction products with a higher volume than that of the solid starting materials, it can be proposed that an analogous reasoning is valid for these materials also; *i.e.*, there will be a theoretical  $w/(\text{CaO} + \text{MgO}_{\text{eq}} + \text{Na}_2\text{O}_{\text{eq}} + \text{K}_2\text{O}_{\text{eq}})$  ratio that leads to depercolation of the capillary pore system, and thus significantly decreased carbonation rates. However, the absolute value of the critical  $w/(\text{CaO} + \text{MgO}_{\text{eq}} + \text{Na}_2\text{O}_{\text{eq}} + \text{K}_2\text{O}_{\text{eq}})$  ratio will strongly depend on the starting materials and the mix design of a specific alkali-activated material, and numerical values have not yet been calculated systematically across the full range of compositions of alkali-activated materials. For GGBS activated by various sodium salts, simulation results [59] indicate that at  $w/b = 0.40$ , a porosity of 18 vol.% is only reached at approx. 90% extent of reaction, so it is expected that rather a low water content will be required to achieve capillary depercolation of AAC in practice, due to the relatively low space-filling character of the key AAC binding phases compared to those in BCC.

A separate plot of  $k_{\text{c-nat}}$  versus  $w/(\text{CaO} + \text{MgO}_{\text{eq}} + \text{Na}_2\text{O}_{\text{eq}} + \text{K}_2\text{O}_{\text{eq}})$  for the GGBS-based AAC (Fig. 6) does not allow a clear correlation to be discerned. This observation that a general correlation

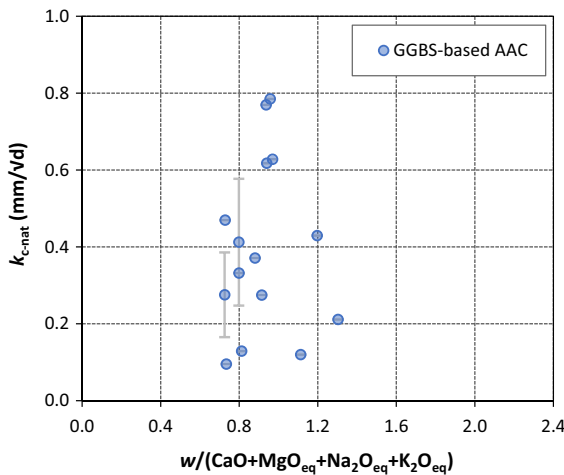


**Fig. 6** Carbonation coefficients of the GGBS-based AAC obtained under conditions approximating natural carbonation (indoor/sheltered) versus  $w/(\text{CaO} + \text{MgO}_{\text{eq}} + \text{Na}_2\text{O}_{\text{eq}} + \text{K}_2\text{O}_{\text{eq}})$  ratio. Error bars represent the estimated s.d. of the results obtained in the round robin testing programme by RILEM TC 247-DTA

between these parameters for the GGBS-based AAC alone cannot be identified, as it is found for all concretes combined, may be related to the fact that particularly for the GGBS-based AAC additional factors can have an important effect on their carbonation resistance; these factors include the role of curing in microstructural development and the formation of alterable carbonate-binding reaction products [5, 11, 22, 23, 26].

Additional parameters were evaluated, including the  $w/b$  ratio of the concretes/mortars; the binder content of the concretes/mortars; the binder paste (binder + water) content of the concretes/mortars; the activator (anhydrous) content of the AAC; the silicate modulus ( $\text{SiO}_2/\text{M}_2\text{O}$ , where  $M = \text{K}$  or  $\text{Na}$ , in mol/mol) of the activator of the AAC; and the Portland clinker content of the BCC. None of these yielded a satisfactory correlation with  $k_{c\text{-nat}}$  for all concretes/mortars combined (Supplementary Figs. S7–S12).

It is noted that for the BCC, correlations were found for  $k_{c\text{-nat}}$  versus  $w/(\text{CaO} + \text{MgO}_{\text{eq}} + \text{Na}_2\text{O}_{\text{eq}} + \text{K}_2\text{O}_{\text{eq}})$  and for  $k_{c\text{-nat}}$  versus  $w/b$  (Supplementary Figs. S5 and S6). However, both coefficients of determination were considerably lower than for the relationship between  $k_{c\text{-nat}}$  and  $w/\text{CaO}$  (Fig. 4). That a correlation between  $k_{c\text{-nat}}$  and  $w/b$  was found can be explained by the fact that GGBS was the major SCM in most of the BCC mixes in the database; thus, for these materials,

$w/\text{CaO}$  is approximately proportional to  $w/b$ . However, since the CaO content of the binders was not identical, the coefficient of determination was lower for  $w/b$  than for  $w/\text{CaO}$ . This result is an additional demonstration of the usefulness of  $w/\text{CaO}$  to predict the carbonation resistance of concretes based on high-volume SCM blended cements.

### 3.2 Accelerated carbonation versus carbonation under conditions approximating natural exposure

Accelerated carbonation testing involves exposing concrete or mortar samples to an atmosphere with a  $\text{CO}_2$  concentration ( $c_{\text{CO}_2}$ ) higher than the natural  $\text{CO}_2$  concentration in air ( $\sim 0.04\%$ ). The advantage of accelerated carbonation testing is that the results are available much earlier than for natural carbonation testing. Assuming that the square root-of-time law holds for estimating the depth of carbonation of concrete [4, 53], the relationship between the carbonation coefficients obtained with accelerated carbonation and natural carbonation can be derived as [60, 61]:

$$\frac{k_{c\text{-acc}}}{k_{c\text{-nat}}} = \sqrt{\frac{c_{\text{CO}_2,\text{acc}}}{c_{\text{CO}_2,\text{nat}}}} \quad (1)$$

where  $c_{\text{CO}_2,\text{acc}}$  is the  $\text{CO}_2$  concentration applied in accelerated carbonation testing, and  $c_{\text{CO}_2,\text{nat}}$  is the natural  $\text{CO}_2$  concentration in air. For example, inserting 1% for  $c_{\text{CO}_2,\text{acc}}$  and 0.04% for  $c_{\text{CO}_2,\text{nat}}$  yields  $k_{c\text{-acc}}[1\%]/k_{c\text{-nat}} = \sqrt{(1/0.04)} = 5$ . It is important to note that this is only applicable when other exposure conditions such as relative humidity and temperature are similar in both natural and accelerated carbonation testing. There are some experimental data supporting at least the approximate validity of Eq. (1) for BCC [6, 61], though the deviations between computed and measured carbonation coefficients can be significant [1, 4, 62, 63]. Whether Eq. (1) holds, at least approximately, for alkali-activated materials has not previously been systematically investigated.

Figure 7 shows that for BCC and GGBS-based AAC, the relationship between  $k_{c\text{-acc}}$  and  $k_{c\text{-nat}}$  appears to generally conform to Eq. (1). Conversely, FA- and MK-based AAC yield considerably lower  $k_{c\text{-acc}}$  than what would be expected from Eq. (1) at  $\text{CO}_2$  concentrations of 1% and in the range 3–4%. The finding that the behaviour of the FA- and MK-based AAC deviates



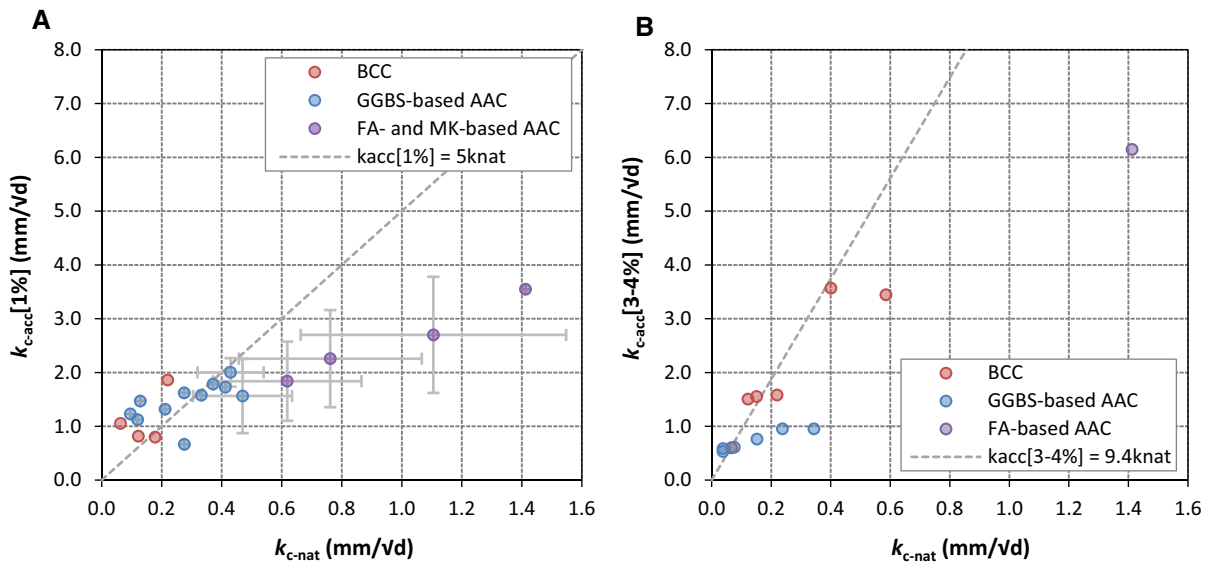


**Fig. 7** Carbonation coefficients obtained under accelerated conditions (**A**,  $c_{\text{CO}_2,\text{acc}} = 1\%$ ; **B**,  $c_{\text{CO}_2,\text{acc}} = 3\text{--}4\%$ ) versus carbonation coefficients obtained under conditions

significantly from the expected relationship between  $k_{\text{c-acc}}$  and  $k_{\text{c-nat}}$  has important implications. Most importantly, it indicates that the outcomes of accelerated carbonation testing of low-Ca alkali-activated materials can lead to inaccurate predictions of their carbonation resistance under natural exposure, as has previously been indicated based on thermodynamic considerations [5]. However, the number of available studies of these materials that include both accelerated and natural carbonation testing results for the same materials is currently very limited (five data points); thus, additional data are required to verify the above conclusion. It is also noted that the testing programme of RILEM TC 247-DTA [8] gave similar relative performance rankings of a diverse set of AAC from natural and accelerated carbonation testing, indicating the usefulness of accelerated testing at least for the purpose of comparison between samples, if not in an absolute sense.

It is noted that an underestimation of the carbonation rate has been observed also for high-volume fly ash (50% fly ash in the binder) concrete and mortar when comparing the carbonation coefficient obtained by testing at  $c_{\text{CO}_2} = 10\%$  with the coefficient obtained at  $c_{\text{CO}_2} = 1\%$  [62], and when comparing the carbonation coefficients obtained at  $c_{\text{CO}_2} = 10\%$  and at  $c_{\text{CO}_2} = 1\%$  with the coefficient obtained at natural

approximating natural carbonation (indoor/sheltered). Error bars represent the estimated s.d. of the results obtained in the round robin testing programme by RILEM TC 247-DTA

$\text{CO}_2$  concentration [63]. This may suggest that Eq. (1) is generally not valid for concretes with a high proportion of SCMs in the binder, though the data for the GGBS-based AAC and the BCC in the present study appear to conform to Eq. (1), possibly in part due to the limited number of data points.

### 3.3 Accelerated carbonation

No relationship between  $k_{\text{c-acc}}$  and  $w/\text{CaO}$  or  $w/(\text{CaO} + \text{MgO}_{\text{eq}})$  of the concretes/mortars was found, no matter which  $\text{CO}_2$  concentration was considered (Supplementary Figs. S13–S18). As above for natural carbonation testing, this is mainly explained by the fact that the  $\text{CO}_2$  binding capacity of AAC is influenced to a large extent by the alkali metals in the pore solution and the binder, usually introduced by the activator.

A comparison of the  $k_{\text{c-acc}}[1\%]$  values and  $w/(\text{CaO} + \text{MgO}_{\text{eq}} + \text{Na}_2\text{O}_{\text{eq}} + \text{K}_2\text{O}_{\text{eq}})$  (Fig. 8) indicates that there is a weak correlation between these parameters. A linear regression of the data, ignoring the data point for the MK-based AAC, yields a coefficient of determination of 0.4332 (Fig. 8), lower than for the correlation between  $k_{\text{c-nat}}$  and  $w/(\text{CaO} + \text{MgO}_{\text{eq}} + \text{Na}_2\text{O}_{\text{eq}} + \text{K}_2\text{O}_{\text{eq}})$ . The obtained linear function yields an intercept with the abscissa

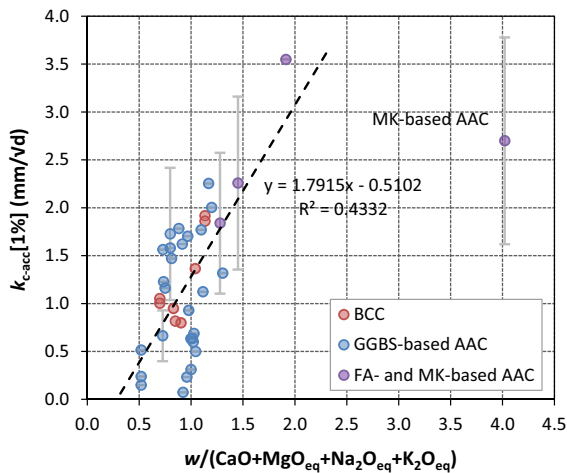


**Fig. 8** Carbonation coefficients obtained with a  $\text{CO}_2$  concentration of 1% (accelerated conditions) versus  $w/(\text{CaO} + \text{MgO}_{\text{eq}} + \text{Na}_2\text{O}_{\text{eq}} + \text{K}_2\text{O}_{\text{eq}})$  ratio. The dashed line is a linear fit through all data points except the MK-based AAC. Error bars represent the estimated s.d. of the results obtained in the round robin testing programme by RILEM TC 247-DTA

(i.e.  $k_{\text{c-nat}} = 0.0 \sqrt{\text{mm/d}}$ ) at  $w/(\text{CaO} + \text{MgO}_{\text{eq}} + \text{Na}_2\text{O}_{\text{eq}} + \text{K}_2\text{O}_{\text{eq}}) = 0.28$ . As discussed above, this finding might be explained by the existence of a theoretical, critical value below which the capillary pore system of the concretes/mortars becomes discontinuous, thus inhibiting the ingress of  $\text{CO}_2$ . However, in accelerated carbonation of AAC, the influence

of any microstructural changes in the binding phases induced by the carbonation reactions would be expected to be more marked than under natural carbonation conditions, and so this critical compositional value for pore network depercolation (discontinuity of the capillary pore system) will become dependent on the testing conditions rather than being a defining material characteristic.

The evident large scatter of the data in Fig. 8 in some ways appears to mask the fact that the  $k_{\text{c-acc}}[1\%]$  obtained for FA- and MK-based AAC do not reflect their carbonation resistance under natural conditions in the same way as is the case for BCC and GGBS-based AAC (Sect. 3.2). Thus, the numerical correlation identified appears to be partly fortuitous, and does not necessarily imply accurate predictive power.

For carbonation testing under higher  $\text{CO}_2$  concentrations ( $c_{\text{CO}_2} \geq 3\%$ ), no correlation between  $k_{\text{c-acc}}$  and  $w/(\text{CaO} + \text{MgO}_{\text{eq}} + \text{Na}_2\text{O}_{\text{eq}} + \text{K}_2\text{O}_{\text{eq}})$  is observed (Fig. 9), indicating that the significance of these tests is limited, and/or that other parameters beyond the scope of the current analysis, such as the microstructural damage noted above, could play a more important role here. It is also possible that this relates to deviations from the assumptions that underpin the use of the square root-of-time relationship to obtain a characteristic coefficient to describe carbonation kinetics for materials that differ significantly

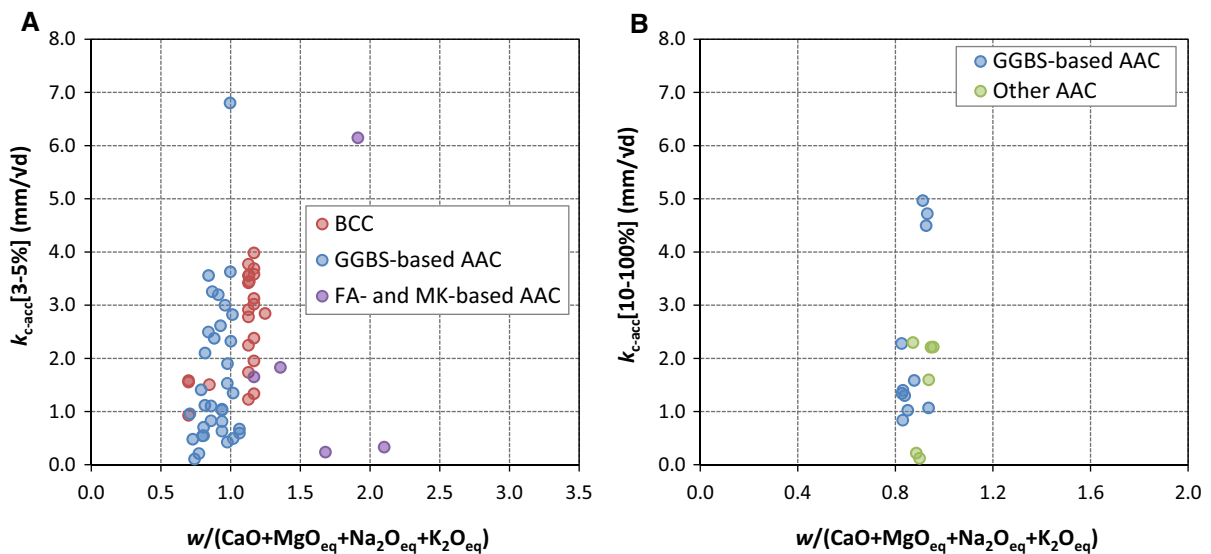


**Fig. 9** Carbonation coefficients obtained with **A**, a  $\text{CO}_2$  concentration in the range 3–5% (accelerated conditions), and **B**, a  $\text{CO}_2$  concentration in the range 10–100% (accelerated conditions), versus  $w/(\text{CaO} + \text{MgO}_{\text{eq}} + \text{Na}_2\text{O}_{\text{eq}} + \text{K}_2\text{O}_{\text{eq}})$  ratio

from plain Portland cement [5, 18, 20]; this merits further investigation. The scope of analysis that is possible for conditions of 10–100% CO<sub>2</sub> (Fig. 9B) is further restricted by the fact that all available data fall into a very narrow range of  $w/(\text{CaO} + \text{MgO}_{\text{eq}} + \text{Na}_2\text{O}_{\text{eq}} + \text{K}_2\text{O}_{\text{eq}})$  values. However, current trends in materials testing are moving away from these very highly accelerated carbonation tests due to their unrealistic impacts on material chemistry and microstructure compared to natural conditions.

Additional parameters were evaluated regarding a correlation with  $k_{\text{c-acc}}$ , including the  $w/b$  ratio of the concretes/mortars, and the silicate modulus of the activator of the AAC. None of these yielded a satisfactory correlation for all concretes/mortars combined (Supplementary Figs. S19–S24).

#### 4 Concluding remarks

The reported data for the carbonation resistance of alkali-activated concretes and mortars are very unevenly distributed: While a comparatively high number of studies concerning GGBS-based AAC were found, only a small number of studies that report the carbonation rate of FA- and MK-based AAC exist. Concerning ‘other AAC’, *i.e.* materials with binders based on municipal solid waste incineration bottom ash, non-ferrous slag or natural pozzolans, and hybrid cements, more data are available, but the majority of these were obtained under highly accelerated carbonation conditions ( $c_{\text{CO}_2} \geq 10\%$ ); thus, these results might not be directly comparable with those obtained under lower CO<sub>2</sub> concentrations. Thus, to better understand the carbonation of alkali-activated binders as a class of cements, *i.e.* over their complete range of chemistries, it will be necessary to obtain more data on the carbonation resistance of FA- and MK-based AAC concretes/mortars (low-Ca alkali-activated materials) as well as concretes based on non-conventional alkali-activated binders, such as natural pozzolans or calcined clays other than MK.

An equally important issue is the comparison of results obtained under accelerated carbonation conditions with results of conditions approximating natural carbonation: While several studies have investigated this issue for Portland cement concretes and BCC, there is only limited data available in this regard for GGBS-based AAC, and only two studies [8, 33] were

found that relate to FA- and MK-based AAC. Thus, future studies should focus on the comparison between the results obtained under accelerated carbonation conditions and conditions approximating natural exposure of these concretes. Though not subject of the present analysis, it appears also necessary to study the effects of relative humidity during carbonation testing in the laboratory and under unsheltered natural conditions, as has been done for conventional (blended) cement concretes [1].

As regards the present results, two findings appear particularly significant in that they have important implications for the design of alkali-activated concretes and tests of their carbonation resistance:

- (1) The carbonation coefficient of GGBS- and FA-based AAC obtained under conditions approximating natural exposure and, by implication, under natural carbonation, appears to be related to their  $w/(\text{CaO} + \text{MgO}_{\text{eq}} + \text{Na}_2\text{O}_{\text{eq}} + \text{K}_2\text{O}_{\text{eq}})$  ratio. This correlation included the high-volume SCM concretes (BCC) in the present database; thus, alkali-activated concretes and high-volume SCM concretes appear to behave similarly at least in this respect. However, the scatter of the pertinent data is considerable; thus, this ratio may serve as a rough indicator of the carbonation resistance at best. Other factors that influence the carbonation resistance of alkali-activated concretes have been studied and discussed in the literature in considerable details, and these factors must be considered in addition when alkali-activated concretes with satisfactory real-world performance are to be designed.
- (2) For FA- and MK-based AAC (low-Ca alkali-activated materials), accelerated carbonation testing at CO<sub>2</sub> concentrations in the range 1–4% leads to considerably lower carbonation coefficients than what would be expected from carbonation testing under conditions approximating natural exposure and the square root-of-time law. Thus, the present data suggests that accelerated carbonation testing combined with the application of the square root-of-time law leads to inaccurate predictions of the actual carbonation resistance of these materials; namely, this approach may lead to underestimated carbonation coefficients (overestimated

carbonation resistance) under real-world conditions. Additional work is required to verify this conclusion and to elucidate the underlying mechanisms. For CO<sub>2</sub> concentrations higher than 1%, the present database shows no correlation with any of the investigated mix design parameters, including  $w/(CaO + MgO_{eq} + Na_2O_{eq} + K_2O_{eq})$ , thus indicating that the establishment of a relationship between these results and the carbonation resistance under natural conditions will be difficult to achieve.

In addition, the present data demonstrate that there is a correlation between the carbonation coefficient of high-volume SCM concretes obtained under conditions approximating natural exposure and their  $w/CaO$  ratio. This finding is in line with previous studies [1, 2, 4] that have shown that the carbonation coefficient of materials based on blended Portland cements obtained under conditions approximating natural exposure is related to their  $w/CaO_{reactive}$  ratio, and it indicates that the  $w/CaO$  ratio of high-volume SCM concretes can serve as a proxy for their  $w/CaO_{reactive}$  ratio.

The above conclusions are based on results obtained using the phenolphthalein-spraying method to determine the carbonation depths of concretes and mortars based on alkali-activated cements or blended cements. As mentioned above, peculiarities of the phenolphthalein-spraying method applied to alkali-activated concretes have been reported [8], and the method relates to the pH of the pore solutions of the analysed concretes and mortars, while the precipitation of carbonates and other processes in the materials cannot be directly analysed with it. Due to the presence of significant concentrations of alkali metal ions in the pore solutions of alkali-activated materials, the main carbonation products and the pore solution compositions of alkali-activated materials differ from those of Portland cement-based materials (see, e.g., refs. [5, 56, 64]). Thus, differences between these materials may also exist as regards the significance of the carbonation depths obtained with the phenolphthalein-spraying method and the influence of CO<sub>2</sub> concentration on these. To fully understand and describe these differences, additional studies are required, the outcomes of which may ultimately motivate a re-evaluation of the present dataset.

Finally, it is noted that the application of data science methods, such as machine learning [65, 66], to the present dataset might yield insights into the carbonation resistance of alkali-activated materials in addition to those obtained in the present analysis. To enable such analyses in future studies, the full dataset underlying the present analysis is provided as Electronic Supplementary Material alongside this article.

**Acknowledgements** Valuable discussion with many of the members of RILEM TC 281-CCC about aspects of the carbonation of concretes in general, and alkali-activated concretes in particular, are gratefully acknowledged.

**Funding** Open Access funding enabled and organized by Projekt DEAL. Participation of S. A. Bernal in this study was sponsored by the Engineering and Physical Sciences Research Council (EPSRC) through the Early Career Fellowship EP/R001642/1, and the National Science Foundation/ EPSRC lead agency RENACEM grant EP/T008407/1 and 1903457. Participation of J. L. Provis in this study was supported by the Engineering and Physical Sciences Research Council through grant EP/T008407/1.

#### Declarations

**Competing of interest** The authors declare no competing interest.

**Open Access** This article is licensed under a Creative Commons Attribution 4.0 International License, which permits use, sharing, adaptation, distribution and reproduction in any medium or format, as long as you give appropriate credit to the original author(s) and the source, provide a link to the Creative Commons licence, and indicate if changes were made. The images or other third party material in this article are included in the article's Creative Commons licence, unless indicated otherwise in a credit line to the material. If material is not included in the article's Creative Commons licence and your intended use is not permitted by statutory regulation or exceeds the permitted use, you will need to obtain permission directly from the copyright holder. To view a copy of this licence, visit <http://creativecommons.org/licenses/by/4.0/>.

#### References

1. Leemann A, Nygaard P, Kaufmann J, Loser R (2015) Relation between carbonation resistance, mix design and exposure of mortar and concrete. *Cem Concr Compos* 62:33–43. <https://doi.org/10.1016/j.cemconcomp.2015.04.020>
2. Leemann A, Moro F (2017) Carbonation of concrete: the role of CO<sub>2</sub> concentration, relative humidity and CO<sub>2</sub> buffer capacity. *Mater Struct* 50:30. <https://doi.org/10.1617/s11527-016-0917-2>



3. von Greve-Dierfeld S, Gehlen C (2015) Performance-based durability design, carbonation part 2 – classification of concrete. *Struct Concr* 17:523–532. <https://doi.org/10.1002/suco.201600067>
4. von Greve-Dierfeld S, Lothenbach B, Vollpracht A, Wu B, Huet B, Andrade C, Medina C, Thiel C, Gruyaert E, Vanoutrive H, Saéz del Bosque IF, Ignjatovic I, Elsen J, Provis JL, Scrivener K, Thienel K-C, Sideris K, Zajac M, Alderete N, Cizer Ö, Van den Heede P, Hooton D, Kamali-Bernard S, Bernal SA, Zhao Z, Shi Z, De Belie N (2020) Understanding the carbonation of concrete with supplementary cementitious materials: a critical review by RILEM TC 281-CCC. *Mater Struct* 53:136. <https://doi.org/10.1617/s11527-020-01558-w>
5. Bernal SA, Provis JL, Brice DG, Kilcullen A, Duxson P, van Deventer JSJ (2012) Accelerated carbonation testing of alkali-activated binders significantly underestimates service life: the role of pore solution chemistry. *Cem Concr Res* 42:1317–1326. <https://doi.org/10.1016/j.cemconres.2012.07.002>
6. Leemann A, Pahlke H, Loser R, Winnefeld F (2018) Carbonation resistance of mortar produced with alternative cements. *Mater Struct* 51:114. <https://doi.org/10.1617/s11527-018-1239-3>
7. Bernal SA, Provis JL (2014) Durability of alkali-activated materials: progress and perspectives. *J Am Ceram Soc* 97:997–1008. <https://doi.org/10.1111/jace.12831>
8. Gluth GJG, Arbi K, Bernal SA, Bondar D, Castel A, Chithiraputhiran S, Dehghan A, Dombrowski-Daube K, Dubey A, Ducman V, Peterson K, Pipilikaki P, Valcke SLA, Ye G, Zuo Y, Provis JL (2020) RILEM TC 247-DTA round robin test: carbonation and chloride penetration testing of alkali-activated concretes. *Mater Struct* 53:21. <https://doi.org/10.1617/s11527-020-1449-3>
9. Provis JL, Arbi K, Bernal SA, Bondar D, Buchwald A, Castel A, Chithiraputhiran S, Cyr M, Dehghan A, Dombrowski-Daube K, Dubey A, Ducman V, Gluth GJG, Nanukuttan S, Peterson K, Puertas F, van Riessen A, Torres-Carrasco M, Ye G, Zuo Y (2019) RILEM TC 247-DTA round robin test: mix design and reproducibility of compressive strength of alkali-activated concretes. *Mater Struct* 52:99. <https://doi.org/10.1617/s11527-019-1396-z>
10. Khan MSH, Castel A (2018) Effect of MgO and Na<sub>2</sub>SiO<sub>3</sub> on the carbonation resistance of alkali activated slag concrete. *Mag Concr Res* 70:685–692. <https://doi.org/10.1680/jmacr.17.00062>
11. Bernal SA, Provis JL, Gutierrez RM, van Deventer JSJ (2015) Accelerated carbonation testing of alkali-activated slag/metakaolin blended concretes: effect of exposure conditions. *Mater Struct* 48:653–659. <https://doi.org/10.1617/s11527-014-0289-4>
12. Law D, Adam A, Molyneaux T, Patnaikuni I (2012) Durability assessment of alkali activated slag (AAS) concrete. *Mater Struct* 45:1425–1437. <https://doi.org/10.1617/s11527-012-9842-1>
13. Bakharev T, Sanjayan JG, Cheng Y-G (2001) Resistance of alkali-activated slag concrete to carbonation. *Cem Concr Res* 31:1277–1283. [https://doi.org/10.1016/S0008-8846\(01\)00574-9](https://doi.org/10.1016/S0008-8846(01)00574-9)
14. Al-Otaibi S (2008) Durability of concrete incorporating GGBS activated by water-glass. *Constr Build Mater* 22:2059–2067. <https://doi.org/10.1016/j.conbuildmat.2007.07.023>
15. Song K-I, Song J-K, Lee BY, Yang K-H (2014) Carbonation characteristics of alkali-activated blast-furnace slag mortar. *Adv Mater Sci Eng* 2014:326458. <https://doi.org/10.1155/2014/326458>
16. Häkkinen T (1993) The influence of slag content on the microstructure, permeability and mechanical properties of concrete. Part 1 Microstructural studies and basic mechanical properties. *Cem Concr Res* 23:407–421. [https://doi.org/10.1016/0008-8846\(93\)90106-J](https://doi.org/10.1016/0008-8846(93)90106-J)
17. Häkkinen T (1993) The influence of slag content on the microstructure, permeability and mechanical properties of concrete. Part 2. Technical properties and theoretical examinations. *Cem Concr Res* 23:518–530. [https://doi.org/10.1016/0008-8846\(93\)90002-Q](https://doi.org/10.1016/0008-8846(93)90002-Q)
18. Bernal SA, San Nicolas R, Provis JL, Mejía de Gutiérrez R, van Deventer JSJ (2014) Natural carbonation of aged alkali-activated slag concretes. *Mater Struct* 47:693–707. <https://doi.org/10.1617/s11527-013-0089-2>
19. Deja J (2002) Carbonation aspects of alkali activated mortars and concretes. *Silic Ind* 67(3–4):37–42
20. Bernal SA, Mejía de Gutierrez R, Pedraza AL, Provis JL, Rodríguez ED, Delvasto S (2011) Effect of binder content on the performance of alkali-activated slag concretes. *Cem Concr Res* 41:1–8. <https://doi.org/10.1016/j.cemconres.2010.08.017>
21. Bernal SA, Provis JL, van Deventer JSJ (2018) Impact of water content on the performance of alkali-activated slag concretes. In: Sixth international conference on the durability of concrete structures, Leeds, United Kingdom, paper No 1302
22. Bernal SA, van Deventer JSJ, Provis J (2019) Natural and accelerated carbonation rates of alkali-activated slag/fly ash blended concretes. In: Barčević A, Rukavina MJ, Damjanović D, Guadagnini M (eds) Proceedings of the international conference on sustainable materials, systems and structures (SMSS 2019), Vol. 3: durability, monitoring and repair of structures. RILEM Publications, Paris, pp 357–364
23. Bernal SA, Mejía de Gutiérrez R, Provis JL, Rose V (2010) Effect of silicate modulus and metakaolin incorporation on the carbonation of alkali silicate-activated slags. *Cem Concr Res* 40:898–907. <https://doi.org/10.1016/j.cemconres.2010.02.003>
24. He J, Gao Q, Wu Y, He J, Pu X (2018) Study on improvement of carbonation resistance of alkali-activated slag concrete. *Constr Build Mater* 176:60–67. <https://doi.org/10.1016/j.conbuildmat.2018.04.117>
25. Bai Y-H, Yu S, Chen W (2019) Experimental study of carbonation resistance of alkali-activated slag concrete. *ACI Mater J* 116:95–104
26. Shi Z, Shi C, Wan S, Li N, Zhang Z (2018) Effect of alkali dosage and silicate modulus on carbonation of alkali-activated slag mortars. *Cem Concr Res* 113:55–64. <https://doi.org/10.1016/j.cemconres.2018.07.005>
27. Behfarnia K, Rostami M (2017) An assessment on parameters affecting the carbonation of alkali-activated slag concrete. *J Clean Prod* 157:1–9. <https://doi.org/10.1016/j.jclepro.2017.04.097>
28. Abdalqader A, Jin F, Al-Tabbaa A (2019) Performance of magnesia-modified sodium carbonate-activated slag/fly ash

- concrete. *Cem Concr Compos* 103:160–174. <https://doi.org/10.1016/j.cemconcomp.2019.05.007>
29. Nedeljković M (2019) Carbonation mechanism of alkali-activated fly ash and slag materials: in view of long-term performance predictions. PhD thesis, Delft University of Technology, The Netherlands
  30. Liu S, Hao Y, Ma G (2021) Approaches to enhance the carbonation resistance of fly ash and slag based alkali-activated mortar – experimental evaluations. *J Clean Prod* 280:124321. <https://doi.org/10.1016/j.jclepro.2020.124321>
  31. Liu G, Florea MVA, Brouwers HJH (2021) The role of recycled waste glass incorporation on the carbonation behaviour of sodium carbonate activated slag mortar. *J Clean Prod* 292:126050. <https://doi.org/10.1016/j.jclepro.2021.126050>
  32. Sufian Badar M, Kupwade-Patil K, Bernal SA, Provis JL, Allouche EN (2014) Corrosion of steel rebars induced by accelerated carbonation in low and high calcium fly ash geopolymer concretes. *Constr Build Mater* 66:179–89. <https://doi.org/10.1016/j.conbuildmat.2014.03.015>
  33. Khan MSH, Castel A, Noushini A (2017) Carbonation of a low-calcium fly ash geopolymer concrete. *Mag Concr Res* 69:24–34. <https://doi.org/10.1680/jmacr.15.00486>
  34. Li Z, Li S (2018) Carbonation resistance of fly ash and blast furnace slag based geopolymer concrete. *Constr Build Mater* 163:668–680. <https://doi.org/10.1016/j.conbuildmat.2017.12.127>
  35. Koenig A, Mahmoud H, Baehre O, Dehn F (2020) Alkalinity and its consequences for the performance of steel-reinforced geopolymer materials. *Molecules* 25:2359. <https://doi.org/10.3390/molecules25102359>
  36. Valencia-Saavedra WG, Aguirre-Guerrero AM, Mejia de Gutiérrez R (2022) Alkali-activated concretes based on high unburned carbon content fly ash: carbonation and corrosion performance. *Eur J Environ Civ Eng* 26:3292–3312. <https://doi.org/10.1080/19648189.2020.1785948>
  37. Huang G, Ji Y, Li J, Hou Z, Jin C (2018) Use of slaked lime and Portland cement to improve the resistance of MSWI bottom ash-GBFS geopolymer concrete against carbonation. *Constr Build Mater* 166:290–300. <https://doi.org/10.1016/j.conbuildmat.2018.01.089>
  38. Huang G, Ji Y, Zhang L, Li J, Hou Z (2018) Advances in understanding and analysing the anti-diffusion behavior in complete carbonation zone of MSWI bottom ash-based alkali-activated concrete. *Constr Build Mater* 186:1072–1081. <https://doi.org/10.1016/j.conbuildmat.2018.08.038>
  39. Navarro R, Alcocel EG, Sánchez I, Garcés P, Zornoza E (2020) Corrosion resistance of steel reinforcements embedded in alkali activated ground granulated SiMn slag mortars. *Constr Build Mater* 230:116917. <https://doi.org/10.1016/j.conbuildmat.2019.116917>
  40. Robayo-Salazar RA, Aguirre-Guerrero AM, Mejia de Gutiérrez R (2020) Carbonation-induced corrosion of alkali-activated binary concrete based on natural volcanic pozzolan. *Constr Build Mater* 232:117189. <https://doi.org/10.1016/j.conbuildmat.2019.117189>
  41. Scholz E, Wierig H-J (1988) Untersuchungen über den Einfluß von Flugaschezusätzen auf das Carbonatisierungsverhalten von Beton I. Ergänzung. Universität Hannover, Institut für Baustoffkunde und Materialprüfung, Hannover
  42. Schießl P, Härdtl R (1992) Untersuchungen an Mörteln und Betonen mit Steinkohlenflugasche für eine erweiterte Anrechenbarkeit der Steinkohlenflugasche, Teile I, II und Dokumentationsband. Forschungsberichte Nr. F 236 und F 323. RWTH Aachen, Institut für Bauforschung, Aachen
  43. Schießl P, Wiens U, Breit W (1994) Reduzierung des Alkalitätsdepots durch Puzzolane. Forschungsbericht Nr. F 397. RWTH Aachen, Institut für Bauforschung, Aachen
  44. Brameshuber W, Rasch S, Uebachs S, Rankers R (2008) Untersuchungen und Abschätzung der Leistungsfähigkeit von Hüttensanden in Bindemittel für Beton. Forschungsbericht Nr. F 7037. RWTH Aachen, Institut für Bauforschung, Aachen
  45. Brameshuber W, Vollpracht A, Rasch S (2009) Erarbeitung von Anwendungsregeln für Hüttensand als Betonzusatzstoff gemäß der harmonisierten europäischen Stoffnorm. Forschungsbericht Nr. F 7038. Fraunhofer IRB Verlag
  46. Brameshuber W, Vollpracht A (2009) Flugaschebetone gleicher Leistungsfähigkeit. Forschungsbericht Nr. F 920. RWTH Aachen, Institut für Bauforschung, Aachen
  47. Brameshuber W, Steinhoff J (2010) Gemeinsame Verwendung von Flugasche und Hüttensand als Zusatzstoff im Beton. Forschungsbericht Nr. F 960/2. RWTH Aachen, Institut für Bauforschung, Aachen
  48. Atis CD (2003) Accelerated carbonation and testing of concrete made with fly ash. *Constr Build Mater* 17:147–152. [https://doi.org/10.1016/S0950-0618\(02\)00116-2](https://doi.org/10.1016/S0950-0618(02)00116-2)
  49. Holthuizen PE, Çopuroğlu O, Polder RB (2018) Chloride ingress of carbonated blast furnace slag cement mortars. *High Tech concrete – where technology and engineering meet*. Springer, Cham, pp 73–82
  50. Gruyaert E, Van den Heede P, De Belie N (2013) Carbonation of slag concrete: effect of the cement replacement level and curing on the carbonation coefficient – effect of carbonation on the pore structure. *Cem Concr Compos* 35:39–48. <https://doi.org/10.1016/j.cemconcomp.2012.08.024>
  51. Angulo-Ramirez DE, Mejía de Gutierrez R, Valencia-Saavedra WG, de Medeiros MHF, Hoppe-Filho J (2019) Carbonation of hybrid concrete with high blast furnace slag content and its impact on structural steel corrosion. *Mater Constr* 69:e182. <https://doi.org/10.3989/mc.2019.05418>
  52. Lee J, Lee T, Choi H, Lee DE (2020) Assessment of optimum CaO content range for high volume FA based concrete considering durability properties. *Appl Sci* 10:6944. <https://doi.org/10.3390/app10196944>
  53. Page CL, Treadaway KWJ (1982) Aspects of the electrochemistry of steel in concrete. *Nature* 297:109–115. <https://doi.org/10.1038/297109a0>
  54. Herterich J, Richardson I, Moro F, Marchi M, Black L (2022) Microstructure and phase assemblage of low-clinker cements during the early stages of carbonation. *Cem Concr Res* 152:106643. <https://doi.org/10.1016/j.cemconres.2021.106643>
  55. Hargis CW, Lothenbach B, Müller CJ, Winnefeld F (2017) Carbonation of calcium sulfoaluminate mortars. *Cem Concr Compos* 80:123–134. <https://doi.org/10.1016/j.cemconcomp.2017.03.003>



56. Pouhet R, Cyr M (2016) Carbonation in the pore solution of metakaolin-based geopolymer. *Cem Concr Res* 88:227–235. <https://doi.org/10.1016/j.cemconres.2016.05.008>
57. Bentz DP, Garboczi EJ (1991) Percolation of phases in a three-dimensional cement paste microstructural model. *Cem Concr Res* 21:325–344. [https://doi.org/10.1016/0008-8846\(91\)90014-9](https://doi.org/10.1016/0008-8846(91)90014-9)
58. Powers TC (1960) Physical properties of cement paste. In: 4th international symposium on the chemistry of cement. US Department of Commerce, Washington DC, USA, vol II, pp 577–609
59. Myers RJ, Lothenbach B, Bernal SA, Provis JL (2015) Thermodynamic modelling of alkali-activated slag cements. *Appl Geochem* 61:233–247. <https://doi.org/10.1016/j.apgeochem.2015.06.006>
60. Papadakis VG, Vayenas CG, Fardis MN (1991) Fundamental modeling and experimental investigation of concrete carbonation. *ACI Mater J* 88:363–373
61. Sisomphon K, Franke L (2007) Carbonation rates of concretes containing high volume of pozzolanic materials. *Cem Concr Res* 37:1647–1653. <https://doi.org/10.1016/j.cemconres.2007.08.014>
62. Van den Heede P, De Belie N (2014) A service life based global warming potential for high-volume fly ash concrete exposed to carbonation. *Constr Build Mater* 55:183–193. <https://doi.org/10.1016/j.conbuildmat.2014.01.033>
63. Van den Heede P, De Belie N (2021) Effects of accelerated carbonation testing on by-product allocation on the CO<sub>2</sub>-sequestration-to-emission ratios of fly ash-based binder systems. *Appl Sci* 11:2781. <https://doi.org/10.3390/app11062781>
64. Babae M, Khan MSH, Castel A (2018) Passivity of embedded reinforcement in carbonated low-calcium fly ash-based geopolymer concrete. *Cem Concr Compos* 85:32–43. <https://doi.org/10.1016/j.cemconcomp.2017.10.001>
65. Li Z, Yoon J, Zhang R, Rajabipour F, Srubar WV III, Dabo I, Radlińska A (2022) Machine learning in concrete science: applications, challenges, and best practices. *NPJ Comput Mater* 8:127. <https://doi.org/10.1038/s41524-022-00810-x>
66. Rios RT, Childs CM, Smith SH, Washburn NR, Kurtis KE (2021) Advancing cement-based materials design through data science approaches. *RILEM Tech Lett* 6:140–149

**Publisher's Note** Springer Nature remains neutral with regard to jurisdictional claims in published maps and institutional affiliations.

